Quark model and equivalent local potential

Sachiko Takeuchi
Japan College of Social Work, Kiyose, Japan

Kiyotaka Shimizu
Department of Physics, Sophia University, Chiyoda-ku, Tokyo, Japan
(Received 13 January 2002; published 31 May 2002)

In this paper, we investigate the short-range repulsion given by the quark cluster model employing an inverse scattering problem. We find that the local potential which reproduces the same phase shifts as those given by the quark cluster model has a strong repulsion at short distances in the $NN\ {}^1S_0$ channel. There, however, appears an attractive pocket at very short distances due to a rather weak repulsive behavior at very high energy. This repulsion-attractive-pocket structure becomes more manifest in the channel which has an almost forbidden state, $\Sigma N(T=3/2)\ {}^3S_1$. In order to see what kinds of effects are important to reproduce the short-range repulsion in the quark cluster model, we investigate the contribution coming from the one-gluon-exchange potential and the normalization separately. It is clarified that the gluon exchange constructs the short-range repulsion in the $NN\ {}^1S_0$ while the quark Pauli-blocking effect governs the feature of the repulsive behavior in the $\Sigma N(T=3/2)\ {}^3S_1$ channel.

DOI: 10.1103/PhysRevC.65.064006 PACS number(s): 13.75.Cs, 12.39.Jh, 03.65.Nk, 02.30.Zz

I. INTRODUCTION

In nucleon-nucleon (NN) scattering, the phase shift becomes negative as the relative energy increases. In order to explain this behavior, the short-range strong repulsion has been introduced in the NN potential [1,2]. In a microscopic model with a meson-exchange potential [3,4], vector-meson exchange has been shown to produce such a short-range strong repulsion. There also have been many studies to investigate the short-range part of the potential by introducing subnucleonic degrees of freedom. Among them, the model called the quark cluster model (QCM) [5–9] is one of the most successful models which can explain the repulsive behavior of the phase shift in baryon-baryon scattering.

The characteristic features of the quark model potential are its nonlocality and energy dependence. The former appears by integrating the internal quark degrees of freedom out while the latter appears when interpreting its nonlocality to the energy dependence. The energy-dependent potential shows that the core increases as the energy increases [10].

By taking parameters to minimize the nucleon mass, the effect of the orbital [42] symmetry to lower the core was found to be diminished [6]. This has been confirmed by a calculation which takes into account not only NN but also $\Delta\Delta$ and CC channels. Therefore it is enough to consider the single-channel problem to discuss the short-range part of the baryon-baryon interaction.

It is known that nonlocal and energy-dependent terms play an important role in producing the repulsive behavior of NN systems in the conventional model [11]. Nonlocality is considered to be important also in the quark model; it has been studied qualitatively employing a simple nonlocal potential [12]. There, they found that the approximation which has usually been used to obtain the energy-dependent local potential from the nonlocal one is actually valid in energy region concerned. Furthermore, it was shown that the equivalent local potential can be obtained from the simple nonlocal potential by solving the inverse scattering problem; namely, they obtained a unique local potential which gives the same phase shifts as the nonlocal potential.

In this paper we employ a realistic baryon potential given by the quark model and solve the inverse scattering problem. In S-wave NN scattering, the norm kernel, which gives a rough estimate of the size of the Pauli-blocking effect, is known to be small. The one-gluon-exchange potential (OGEP) appearing together with the quark exchanges, however, is large and highly nonlocal in this channel.

On the other hand, there are some channels where the norm kernel becomes very small. In this case we expect that there appears a large repulsive interaction due to the Pauli blocking effect [13]. In order to look into these two effects in detail, we study two typical channels, $NN\ {}^1S_0$ and $\Sigma N(T=3/2)\ {}^3S_1$, and investigate each contribution coming from OGEP and the norm kernel separately.

In the next section we explain briefly the quark cluster model. The method to obtain the baryon potential from QCM (the QCM potential) is also discussed. In Sec. III, we explain the inverse scattering problem; we use this method to derive the energy-independent local potential which reproduces the same phase shifts as those obtained from the QCM potential. We explain two types of quark cluster models in Sec. IV. One is called the OGEP quark model, where the OGEP plays the dominant role in reproducing the mass difference between the nucleon and Δ, and also to produce the NN short-range repulsion. The other is the hybrid chiral (HC) quark model where the pseudoscalar- and scalar-meson-exchange potentials between quarks including quark exchanges are taken into account together with the OGEP. Numerical results are given in Sec. V. It is shown that the obtained local potential has a strong short-range repulsion. It however also has an attractive pocket at very short distances which reflects the fact that the nonlocal repulsion becomes weaker as the energy increases. It is also shown that the channel which has an almost forbidden state has such a structure in a more exten-

sive way. Also, nonlocality seems to become more important there. A summary is given in Sec. VI.

II. QUARK CLUSTER MODEL

Here we briefly summarize the quark cluster model to study the baryon-baryon scattering in terms of the constituent quarks.

The total wave function of the six quark system is given by

$$\Psi(\boldsymbol{\xi}_A,\boldsymbol{\xi}_B,\boldsymbol{R}_{AB})=\mathcal{A}[\phi_A(\boldsymbol{\xi}_A)\phi_B(\boldsymbol{\xi}_B)\chi(\boldsymbol{R}_{AB})], \tag{1}$$

where ϕ_A and ϕ_B are the single-baryon wave function for baryons A and B. They are given by a product of orbital, flavor-spin, and color parts as

$$\phi(\boldsymbol{\xi})=\varphi(\boldsymbol{\xi})S([3]_{f\sigma})C([111]_c). \tag{2}$$

The $\boldsymbol{\xi}_A$ and $\boldsymbol{\xi}_B$ are internal coordinates of the baryon A and B, χ is the relative wave function, $\boldsymbol{R}_{AB}$ is the relative coordinate between the baryons A and B, and $\mathcal{A}$ is the antisymmetrization operator among six quarks. Assuming that the internal wave function $\phi(\boldsymbol{\xi})$ is known, we obtain the following resonating group method (RGM) equation to determine the relative wave function χ,

$$\int H(\boldsymbol{R},\boldsymbol{R}')\chi(\boldsymbol{R}')d\boldsymbol{R}'=E\int N(\boldsymbol{R},\boldsymbol{R}')\chi(\boldsymbol{R}')d\boldsymbol{R}', \tag{3}$$

where H and N are the Hamiltonian and normalization kernels:

$$\begin{Bmatrix} H(\boldsymbol{R},\boldsymbol{R}') \\ N(\boldsymbol{R},\boldsymbol{R}') \end{Bmatrix}=\int d\boldsymbol{\xi}_A d\boldsymbol{\xi}_B d\boldsymbol{R}_{AB}\phi_A^\dagger(\boldsymbol{\xi}_A)\phi_B^\dagger(\boldsymbol{\xi}_B)\delta(\boldsymbol{R}-\boldsymbol{R}_{AB}) \times\begin{Bmatrix} H \\ 1 \end{Bmatrix}\mathcal{A}[\phi_A(\boldsymbol{\xi}_A)\phi_B(\boldsymbol{\xi}_B)\delta(\boldsymbol{R}'-\boldsymbol{R}_{AB})]. \tag{4}$$

Employing the Gaussian

$$g(\boldsymbol{r},b)=(\sqrt{\pi}b)^{-3/2}\exp\{-r^2/(2b^2)\}, \tag{5}$$

we take the orbital part of the internal wave function $\varphi(\boldsymbol{\xi})$ as

$$\varphi(\boldsymbol{\xi})=g(\boldsymbol{\xi}_1,\sqrt{2}b)g(\boldsymbol{\xi}_2,\sqrt{3/2}b), \tag{6}$$

where

$$\boldsymbol{\xi}=(\boldsymbol{\xi}_1,\boldsymbol{\xi}_2)=\begin{cases} \left(\boldsymbol{r}_1-\boldsymbol{r}_2,\dfrac{\boldsymbol{r}_1+\boldsymbol{r}_2}{2}-\boldsymbol{r}_3\right) & \text{for } A, \\ \left(\boldsymbol{r}_4-\boldsymbol{r}_5,\dfrac{\boldsymbol{r}_4+\boldsymbol{r}_5}{2}-\boldsymbol{r}_6\right) & \text{for } B. \end{cases} \tag{7}$$

In this case, the norm kernel is given by the equation

TABLE I. Coefficients of $l=$ even state.

BB	$\langle P_{36}^{(f\sigma c)}\rangle$	$1-9\langle P_{36}^{(f\sigma c)}\rangle$
$NN\ {}^1S_0$	$-\frac{1}{81}$	$\frac{10}{9}$
$\Sigma N(T=3/2)\ {}^3S_1$	$\frac{7}{81}$	$\frac{2}{9}$

$$N(\boldsymbol{R},\boldsymbol{R}')=\delta(\boldsymbol{R}-\boldsymbol{R}')-9\langle P_{36}^{(f\sigma c)}\rangle\left(\frac{27}{16\pi b^2}\right)^{3/2} \times\exp\left[-\frac{15}{16b^2}(R^2+R'^2)+\frac{9}{8b^2}\boldsymbol{R}\cdot\boldsymbol{R}'\right] \tag{8}$$

$$=\sum_{n,l=0}^{\infty}\left[1-9\langle P_{36}^{(f\sigma c)}\rangle\left(\frac{1}{3}\right)^{2n+l}\right]\sum_{m=-l}^{l}u_{nlm}(\boldsymbol{R})u_{nlm}(\boldsymbol{R}')^*, \tag{9}$$

where $u_{nlm}(\boldsymbol{R})$ is the nlm harmonic oscillator wave function with size parameter $\sqrt{2/3}b$, and $P_{36}^{(f\sigma c)}$ is the permutation operator of the third and sixth quarks in the flavor, spin, and color spaces. The expectation values of the permutation operator $P_{36}^{(f\sigma c)}$ are recited in Table I for each of the $NN\ {}^1S_0$ and the $\Sigma N(T=3/2)\ {}^3S_1$ channels.

To see the rough size of the quark effects on the spin-flavor-independent observables, it is useful to see the matrix element of the exchange operator in the flavor-spin-color space. This corresponds to the normalization of the relative $0s$ state, which is affected most largely by the internal degrees of freedom. As seen from Table I, we expect that the effect of Pauli blocking is not important for the $NN\ {}^1S_0$ channel, because the factor $(1-9\langle P_{36}^{(f\sigma c)}\rangle)$ is 10/9, which is close to 1. On the other hand, the factor is 2/9, much smaller than 1, in the $\Sigma N(T=3/2)\ {}^3S_1$ channel. Suppose this factor is found to be zero; it indicates that there is a forbidden state in the concerning channel. Thus, the $0s$ state in the $\Sigma N(T=3/2)\ {}^3S_1$ channel can be called an almost-forbidden state. We will later discuss the role of this almost-forbidden state on the phase shift and the equivalent local potential.

Here we present two ways to rewrite the RGM equation (3) as the ''Schrödinger equation.'' One is to put the exchange part of the norm kernel into the Hamiltonian; the other is to divide the equation by the norm kernel. We explain them in the following.

The norm kernel and Hamiltonian kernel can be decomposed as

$$N=1+N_{ex}, \tag{10}$$

$$H=K_d+K_{ex}+V, \tag{11}$$

where N_{ex} is the exchange part of the norm kernel, and K_d and K_{ex} are direct and exchange parts of the kinetic energy, respectively. The potential V is a part due to the quark-quark potential term together with the quark exchanges. The RGM equation (3) can be written as the Schrödinger equation: viz.,

$$H_s\chi=E\chi,\quad H_s=H-EN_{ex}. \tag{12}$$

Since the K_{ex} and V are highly nonlocal due to the quark exchanges, the Hamiltonian H_s becomes nonlocal as well as energy dependent.

In order to avoid the energy-dependent Hamiltonian, we can rewrite the RGM equation in a different way:

$$H\chi = EN\chi \rightarrow \frac{1}{\sqrt{N}} H \frac{1}{\sqrt{N}} \sqrt{N}\chi = \sqrt{N}\chi. \tag{13}$$

Then the Schrödinger equation becomes

$$\tilde{H}\psi = E\psi. \tag{14}$$

Here the energy-independent Hamiltonian $\tilde{H}$ is defined in the following way:

$$\tilde{H} = \frac{1}{\sqrt{N}} H \frac{1}{\sqrt{N}} \tag{15}$$

$$= K_d + \tilde{V}_{QCM}, \tag{16}$$

where

$$\tilde{V}_{QCM} = \left(\frac{1}{\sqrt{N}} (K_d + K_{ex}) \frac{1}{\sqrt{N}} - K_d \right) + \frac{1}{\sqrt{N}} V \frac{1}{\sqrt{N}}. \tag{17}$$

$\tilde{V}_{QCM}$ can be considered as the potential term in the usual Schrödinger equation for the baryon-baryon scattering, which is very nonlocal, but not energy dependent. The RGM wave function can be obtained from ψ as $\chi = N^{-1/2}\psi$.

Equations (3), (12), and (14) are equivalent to among each other provided that $N^{-1/2}$ is well defined. Their phase shifts are the same and give the same equivalent local potential, which we will discuss in the next section. Though the former treatment is more intuitive, the obtained potential depends strongly on the energy [14]. When looking into the nonlocality of the potential, the latter treatment has an advantage that it does not depend on the energy.

The origin of the short-range repulsion has been argued to come from the quark potential and/or the quark Pauli principle; which of these two reasons is more important depends on the channel. The effect of the nonlocal potential has been discussed employing the simplified model in Ref. [12]. As for the effect of the Pauli principle, we expect that the normalization $\langle N \rangle$ gives a rough estimate. In the channel where $\langle P_{36}^{(f\sigma c)} \rangle$ is positive, $\langle N^{ex} \rangle$ is negative, which causes a repulsion in the short-range part of the potential $\tilde{V}_{QCM}$. This can be understood like this: negative $\langle N_{ex} \rangle$ means that the short-range parts are partially forbidden by the quark Pauli principle. When the wave function is expanded by the harmonic oscillator as in Eq. (9), this effect appears mainly in the $n=0$ component, because the effect is reduced by a factor of $(\frac{1}{9})^n$. The effect appears not only in the normalization but also in the kinetic energy part. Then the diagonal part of the effective kinetic energy $(1/\sqrt{N})(K_d + K_{ex})(1/\sqrt{N})$ remains the same as that of K_d, but the nondiagonal part becomes weaker. As a result the mixing between $0l$ and $1l$ components becomes smaller and so the energy for the $0l$ state becomes higher than the one in the case of $N_{ex}=0$ [15]. See Appendix B.

Since the $\langle N^{ex} \rangle$ is positive in the NN $^1S_0$ channel, we expect that the effect of the Pauli principle does not produce the short-range repulsion there. There exist some channels which have a large negative $\langle N^{ex} \rangle$, such as the $\Sigma N(T=3/2)$ $^3S_1$ channel as shown in Table I.

III. ENERGY-INDEPENDENT LOCAL POTENTIAL

In this section, we apply the inverse scattering method [16,17] to obtain the energy-independent local potential which gives the same phase shifts given by the quark cluster model. This equivalent local potential shows us a more intuitive picture of the nature of this nonlocal potential. Since we are mainly interested in the short-range behavior of the potential, we look only into the S-wave scattering here.

All the information on the scattering observables is in the S matrix $S(k)$. Once $S(k)$ is known, the potential $V(r)$ is obtained by the following equation called the Marchenko equation [16,17]. First we calculate the following $F(r)$ from the S matrix with poles at $\{k = i\kappa_j\}$,

$$F(r) = -\frac{1}{2\pi} \int_{-\infty}^{+\infty} e^{ikr} \{S(k) - 1\} dk + \sum_{\text{all } \kappa_j > 0} c_j^2 e^{-\kappa_j r}, \tag{18}$$

where c_j^2 is

$$c_j^2 = \text{residue}\{S(k)\} \quad \text{at} \quad k = i\kappa_j (\kappa_j > 0). \tag{19}$$

Next we solve the following integral equation using the $F(r)$:

$$K(r,r') = -F(r+r') - \int_r^\infty F(r+r'') K(r,r'') dr''. \tag{20}$$

Then the potential $V(r)$ is given by

$$2\mu V(r) = -2\frac{d}{dr} K(r,r), \tag{21}$$

where μ is the reduced mass for the baryon-baryon scattering.

Provided that the potential is local, the potential V in Eq. (21) can be constructed uniquely from the given S matrix. Also, for any local potentials V_1, V_2, and $V = V_1 + V_2$, suppose we obtain the S matrix for each potential and reconstruct V_1', V_2', and V' by this method; then, $V' = V_1' + V_2'$ holds because $V = V'$, etc., hold. This is not the case if one of V_i is nonlocal. When $V' \sim V_1' + V_2'$ holds, we call these potentials "additive" and use the deviation $V' - (V_1' + V_2')$ as the rough estimate of the degrees of the nonlocality later in Sec. V C.

This method has been applied on the baryon-baryon scattering employing the simple Gaussian-type nonlocal potential [12]. In this paper, we employ this method to the QCM potential, which will be defined in the next section. The procedure is (1) to obtain the S matrix $S(k)$ from the QCM potential up to very high momentum ($k \sim 15$ fm^{-1}) and (2)

to construct a local potential from the S matrix by using Eqs. (18)–(21). See Appendix A for details.

IV. QUARK MODEL HAMILTONIAN

The Hamiltonian of the nonrelativistic quark model [18] is the sum of the kinetic energy and two-body interaction:

$$H^q=\sum_i \left(m_i+\frac{\boldsymbol{p}_i^2}{2m_i}\right)-K_{\rm c.m.}+V^q, \tag{22}$$

where $K_{\rm c.m.}$ is the kinetic energy of the center of mass motion. The two-body potential V^q may consist of the pseudoscalar- and scalar-meson-exchange potentials as well as of the confinement and one-gluon exchange potential. These potentials have been employed to describe the single baryon structure [19]. The color-magnetic part of the OGEP [20] is known to reproduce the mass difference between octet and decuplet baryons. On the other hand, the chiral quark model [21] includes the pseudoscalar meson-exchange potentials, which also contribute to the mass difference. The pseudoscalar mesons appear as Goldstone bosons together with their chiral partner σ meson.

In the following, we employ two types of quark models. One is the OGEP quark model for the baryon-baryon scattering, where only the long-range parts of the meson-exchange potentials are included in addition to the OGEP. The other one is the hybrid chiral quark model, where the pseudoscalar- and scalar-meson exchanges occur between quarks. Thus the potential V^q becomes

$$V^q=\sum_{i>j} V_{ij}=V_{ij}^{conf}+V_{ij}^{OGEP}+V_{ij}^{\sigma}+V_{ij}^{ps}. \tag{23}$$

The explicit form for each potential is as follows. We take the two-body confinement term

$$V_{ij}^{conf}(\boldsymbol{r}_{ij})=-\boldsymbol{\lambda}_i\cdot\boldsymbol{\lambda}_j a_c r_{ij}^2, \tag{24}$$

where $\boldsymbol{\lambda}_i$ is the color SU(3) generator of the ith quark. The OGEP consists of the color Coulomb, electric, and magnetic terms:

$$V_{ij}^{OGEP}(\boldsymbol{r}_{ij})=\boldsymbol{\lambda}_i\cdot\boldsymbol{\lambda}_j\frac{\alpha_s}{4}\left\{\frac{1}{r_{ij}}-\xi_{ij}\frac{\pi}{m^2}\left(1+\frac{2}{3}\boldsymbol{\sigma}_i\cdot\boldsymbol{\sigma}_j\right)\delta(\boldsymbol{r}_{ij})\right\}. \tag{25}$$

Here we have introduced the flavor SU(3) breaking factor ξ_{ij}. This factor takes the following values:

$$\xi_{ij}=\begin{cases} 1 & \text{for } i,j\neq s \text{ quark},\\ \xi_1 & \text{for } i \text{ or } j=s \text{ quark},\\ \xi_2 & \text{for } i \text{ and } j=s \text{ quark}.\end{cases} \tag{26}$$

The parameters ξ_1 and ξ_2 are fixed so as to reproduce the empirical octet baryon masses. The following scalar- and pseudoscalar-meson-exchange potentials are taken into account:

TABLE II. Parameters of OGEP quark model (OGEP) and hybrid chiral quark model (HC).

OGEP and HC							
	Mass (in MeV)					Scale (in fm^{-1})	
m	m_σ	m_π	m_K	m_η		b	Λ
313	675	139	494	547		0.6	4.2
	α_s	ξ_1	ξ_2	a_c [MeV/fm^2]		$g_c^2/4\pi$	$g_\sigma^2/4\pi$
OGEP	1.517	0.603	0.110	26.6		0.592	0.782
HC	1.003	0.683	0.258	11.6		0.592	0.956

$$V_{ij}^{\sigma}(\boldsymbol{r}_{ij})=-\frac{g_\sigma^2}{4\pi}\frac{\Lambda^2}{\Lambda^2-m_\sigma^2}\left(\frac{e^{-m_\sigma r_{ij}}}{r_{ij}}-\frac{e^{-\Lambda r_{ij}}}{r_{ij}}\right), \tag{27}$$

$$V_{ij}^{ps}(\boldsymbol{r}_{ij})=\frac{1}{3}\frac{g_c^2}{4\pi}\frac{m_{ps}^2}{4m^2}\frac{\Lambda^2}{\Lambda^2-m_{ps}^2}\boldsymbol{f}_i\cdot\boldsymbol{f}_j\boldsymbol{\sigma}_i\cdot\boldsymbol{\sigma}_j \times\left\{\frac{e^{-m_{ps}r_{ij}}}{r_{ij}}-\left(\frac{\Lambda}{m_{ps}}\right)^2\frac{e^{-\Lambda r_{ij}}}{r_{ij}}\right\}. \tag{28}$$

We introduce the cutoff Λ for the meson-exchange potentials. The SU(3)-octet pseudoscalar mesons π, K, and η are included.

Both of the models we employ include a few parameters. In the OGEP quark model, the quark mass m and size parameter b are taken to be 313 MeV and 0.6 fm. The quark-gluon coupling constant α_s and confinement strength a_c are fixed by the nucleon and Δ mass difference and the stability condition for the nucleon against the variation of the size parameter b [6]. The long-range parts of the meson-exchange potentials are included as an interaction between baryons added to the potential term in Eq. (14) in order to reproduce the phase shifts at low energies. The quark-σ-meson coupling constant is adjusted to reproduce the $NN\ {}^1S_0$ scattering phase shift at the peak. These parameters are given in Table II. In the table the coupling constants of the meson-exchange potentials are given in terms of the meson-quark coupling; the baryon-meson coupling constant can be calculated from the meson-quark coupling constant and the quark distribution in the baryon.

In the HC quark model, the quark-gluon coupling constant α_s is fixed to reproduce the nucleon and Δ mass difference together with the pseudoscalar-meson-exchange potentials [21,22]. Note that the coupling constant α_s becomes smaller than the one in the OGEP quark model because pseudoscalar-meson exchange also contributes to the mass difference. The quark-exchange terms for the meson-exchange potentials are also included. The parameters used in the present model are also given in Table II.

The coupling constant α_s is determined to reproduce the mass difference between the nucleon and the Δ particle by employing the single-Gaussian wave function. Therefore, OGEP here should be considered as the effective interaction, and its coupling constant is larger than the one given by an analysis of heavy quark system. It has been reported that the

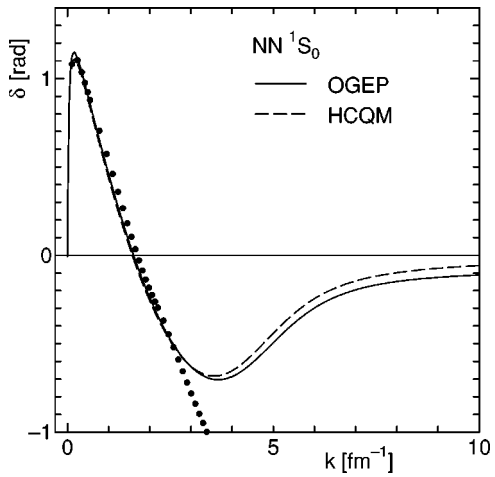

FIG. 1. Phase shifts for the $NN\ ^1S_0$ channel. Dots are experimental values. OGEP and HCQM stand for the OGEP quark model, where only gluon exchange is considered between quarks, and the HC quark model, where the pseudoscalar and scalar meson exchanges are also included between quarks, respectively.

value becomes smaller when the refined wave function is employed, for example, in [23].

V. RESULTS

A. Phase shifts and equivalent local potential

In this section, we show the numerical results of the scattering phase shifts and their equivalent local potentials.

First we show the results of the phase shift for the $NN\ ^1S_0$ channel in Fig. 1 together with the observed phase shift. We employ the OGEP and HC quark models to obtain the QCM phase shifts. Both models reproduce the phase shifts up to momentum $k=2.5$ fm^{-1}. Both phase shifts, however, go to zero rapidly when k becomes beyond about 5 fm^{-1}. As will be seen later, this weak repulsive behavior at high energies partially originated from the nonlocality of the potential.

In Fig. 2, the phase shift for the $\Sigma N(T=3/2)\ ^3S_1$ channel

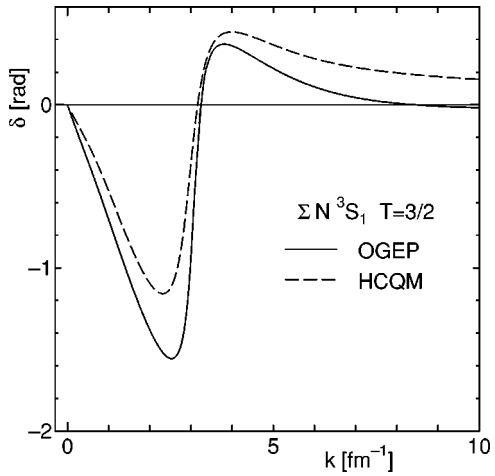

FIG. 2. Phase shifts for the $\Sigma N(T=3/2)\ ^3S_1$ channel. For further explanations see Fig. 1.

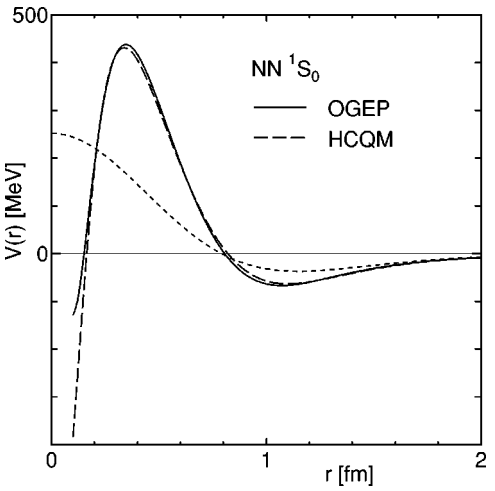

FIG. 3. Equivalent local potential for the $NN\ ^1S_0$ channel using the OGEP or HCQM models. The dotted line indicates the local part of the quark model potential in the OGEP model.

is shown. From the figure, we see that there exists a strong repulsion even at low energies. This is due to a smallness of the norm kernel in this channel. Though the original quark potential is different, the OGEP quark model and HC quark model give results similar to each other.

In Figs. 3 and 4, we show the results of the equivalent local potential given by solving the inverse scattering problem. There, dotted lines denote the local part of the original potential of the OGEP quark model. We see that the nonlocal part of the quark model potential plays an important role especially at short distances. It is noteworthy that there is a very-short-range attraction in addition to the usual short-range repulsion in both channels. This reflects the fact that the nonlocal part, which is repulsive in the intermediate region, is reduced effectively in the very-high-energy region. In the NN system, some of the conventional soft-core models give a similar attraction [24]. This property is more manifest in the $\Sigma N(T=3/2)\ ^3S_1$ channel. There, the very-short-range attraction is due to the existence of the almost forbidden state, which will be discussed later in more details.

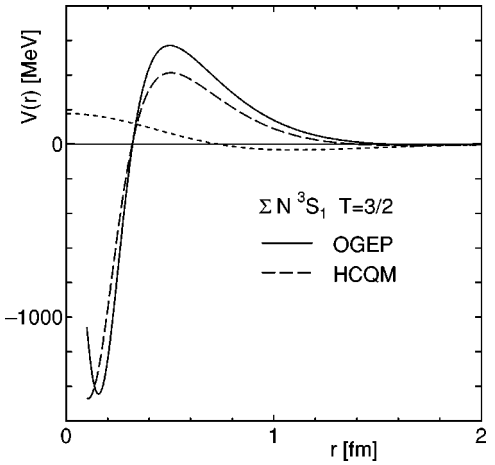

FIG. 4. Equivalent local potential for the $\Sigma N(T=3/2)\ ^3S_1$ channel. For further explanations see Fig. 3.

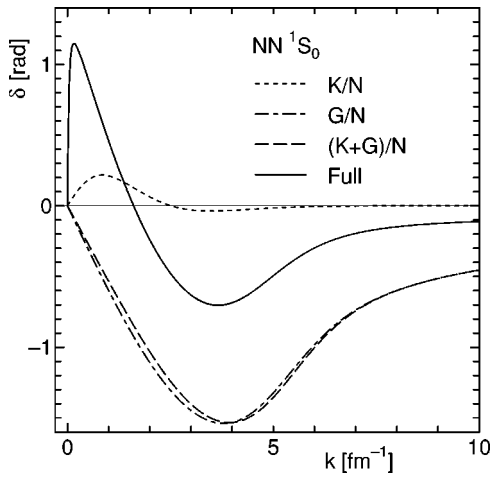

FIG. 5. Calculated phase shifts for the $NN\ ^1S_0$ channel in the OGEP quark model. K/N denotes the contribution from the normalization and kinetic energy terms, G/N denotes the contribution from the normalization and OGEP terms, and $(K+G)/N$ is the contribution from the normalization, kinetic energy, and OGEP terms. ''Full'' is the contribution from $(K+G)/N$ and the meson-exchange potential V_m.

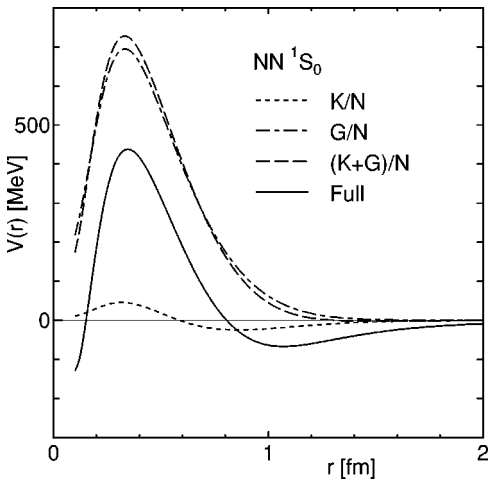

FIG. 6. Equivalent local potential for the $NN\ ^1S_0$ channel in the OGEP quark model. For further explanations see Fig. 5.

B. Roles of the norm kernel and OGEP

In order to see what kinds of effects are important to produce the short-range repulsive interaction in the quark cluster model, we investigate contributions from norm kernel and OGEP separately in the OGEP model. The potential term in the OGEP quark model in Eq. (14) can be rewritten as

$$V=\tilde{V}_{QCM}+V_m, \tag{29}$$

$$\tilde{V}_{QCM}=\tilde{V}_{K/N}+\tilde{V}_{G/N}, \tag{30}$$

$$\tilde{V}_{K/N}=\frac{1}{\sqrt{N}}(K_d+K_{ex})\frac{1}{\sqrt{N}}-K_d, \tag{31}$$

$$\tilde{V}_{G/N}=\frac{1}{\sqrt{N}}V_{OGEP}\frac{1}{\sqrt{N}}. \tag{32}$$

We denote the above three terms as K/N for $\tilde{V}_{K/N}$, G/N for $\tilde{V}_{G/N}$, and V_m in the figures. Note that the meson-exchange term is taken into account as the baryon-baryon interaction in the OGEP quark model.

We first show the calculated phase shift from this potential for the $NN\ ^1S_0$ channel in Fig. 5. Here each contribution from K/N or G/N is shown. We see that the contribution from the norm kernel K/N is rather weak and attractive at low energies. This is because of a small enhancement of the norm kernel due to the quark exchange as seen in Table I [7,8,15]. The contribution from the the OGEP, namely, G/N, is strongly repulsive, and the contribution from both terms, $(K+G)/N$, is almost the same as G/N. Therefore we can conclude that the most important term to reproduce the short-range repulsion in the $NN\ ^1S_0$ channel is the OGEP. When the meson-exchange potential V_m is taken into account, the phase shift becomes positive at low energies as shown by the solid line (denoted as ''Full'' in the figure).

Employing the calculated phase shifts shown in Fig. 5, the equivalent local potential is calculated for $NN\ ^1S_0$ by solving the inverse scattering problem. The results are shown in Fig. 6. As seen in the figure, there exists a strong repulsion due to the norm and OGEP terms, G/N, at short distances. It, however, becomes weak at very short distances; there appears an attractive pocket at short distances. By including the meson-exchange potential consisting of σ, π, and η meson-exchange potentials, the long-range part of the potential becomes attractive.

The results for the $\Sigma N(T=3/2)\ ^3S_1$ channel are shown in Figs. 7 and 8 by employing the OGEP quark model. The reason why we are interested in this channel is that there exists the almost-forbidden state; we can study the role of the Pauli-blocking effect more clearly in this channel. In Fig. 7, we show the contributions from K/N, G/N, $(K+G)/N$, and ''Full'' calculations which includes the meson-exchange potential V_m. As seen in the figure, K/N gives the negative phase shift in the low-energy region, which indicates strong

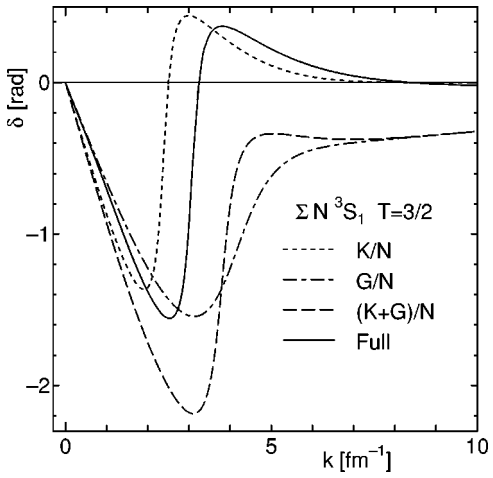

FIG. 7. Calculated phase shifts for the $\Sigma N(T=3/2)\ ^3S_1$ channel in the OGEP quark model. For further explanations see Fig. 5.

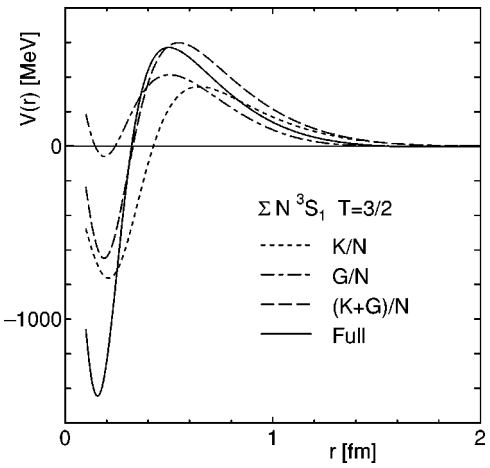

FIG. 8. Equivalent local potential for the $\Sigma N(T=3/2)$ $^3S_1$ channel in the OGEP quark model. For further explanations see Fig. 5.

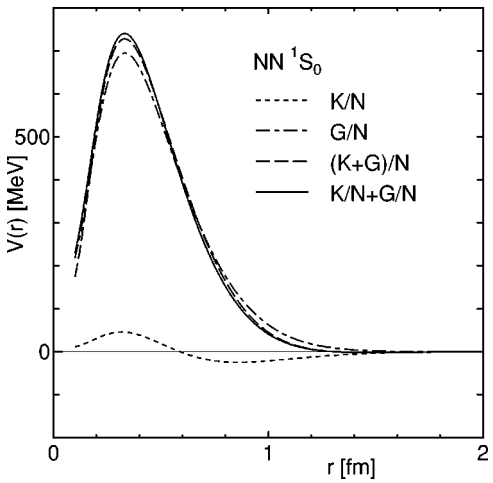

FIG. 9. Equivalent local potential for the NN $^1S_0$ channel in the OGEP quark model. $(K+G)/N$ and $K/N+G/N$ are shown for a comparison. For further explanations see Fig. 5.

repulsion at long ranges. It is also interesting to see that the phase shifts increase sharply around $k\sim 2-4$ fm^{-1}. These are due to the Pauli-blocking effect, because this sharp increase of the phase shift is seen in the cases which include the K/N. Since $\langle P_{36}^{(f\sigma c)}\rangle$ is $\frac{7}{81}$ in this channel, the $0s$ component of the norm kernel is reduced by a factor of $1-7/9=2/9$. Similarly, the $0s$-$1s$ off-diagonal component of the kinetic term and the $0s$ diagonal component are reduced by this factor of 2/9. After being divided by the norm kernel, the diagonal parts of the kinetic energy term K/N are not reduced, but the $0s$-ns nondiagonal parts are reduced by a factor of $\sqrt{2/9}$. This smaller-than-1 factor causes less mixing between the $0s$-$1s$ component. Thus, the K/N term has a node in the phase shift with the repulsion in the lower-energy region [15]. See Appendix B, where this mechanism is imitated by a simple model. Suppose the factor is zero, indicating that the system has a forbidden state; the phase shift decreases continuously toward $-\pi$ at $k=\infty$ in order to satisfy Levinson's theorem.

This feature is also seen in the equivalent local potential shown in Fig. 8. In the equivalent local potential, there appears a very strong attractive potential at short distances with a strong repulsion in the intermediate range. There is a quasibound state in this attractive pocket, which corresponds to the sharp increase of the phase shift. If the factor were zero, the resonance would become a bound state, which is the way to simulate a forbidden state in terms of a local potential because all other real states are forced to be orthogonal to the bound state.

The attraction of the local potential at short distances here simulates the Pauli-blocking effect. This local potential can reproduce the same phase shifts to those given by the original nonlocal potential. The off-shell behaviors of these on-shell equivalent potentials, however, may be quite different from each other when the original potential has a high nonlocality. Therefore, it may be dangerous to apply the local potential with this short-range attraction on the structure calculation, such as the G matrix, and discuss the effects of the attractive pocket of the local potential. The original nonlocal potential should be employed for such a purpose in the channel with an almost-forbidden state.

C. Roles of nonlocality

In order to estimate the degrees of the nonlocality, we investigate whether the contributions from K/N, G/N, and V_m are additive or not. Each local potential given by solving the inverse scattering and their sum are plotted in Figs. 9 and 10. In Fig. 9, we see that the sum of local potentials $V'_{K/N}+V'_{G/N}$ (solid line) is similar to $V'_{(K+G)/N}$ (dashed line), so the nonlocality is weak as we mentioned in the end of Sec. III. By including the meson-exchange potential, $V'_{(K+G)/N}+V_m$ (dot-dashed line) are also compared to $V'_{(K+G)/N+m}$ (solid line) in Fig. 10. As seen in these figures, the equivalent local potentials given by solving the inverse scattering problem are almost additive in the NN $^1S_0$ channel. This suggests that the nonlocality of the QCM potential is rather weak in

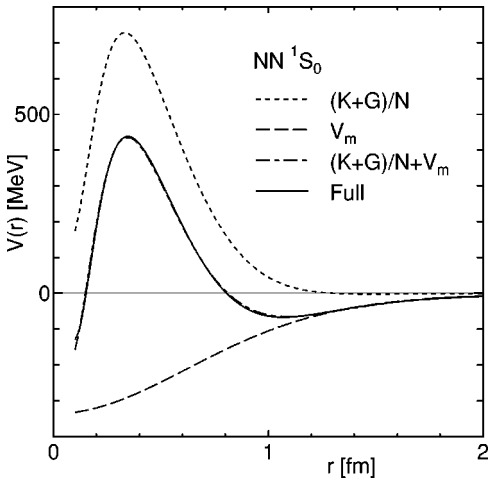

FIG. 10. Equivalent local potential for the NN $^1S_0$ channel in the OGEP quark model. $(K+G)/N+V_m$ and "Full" are shown for a comparison. For further explanations see Fig. 5.

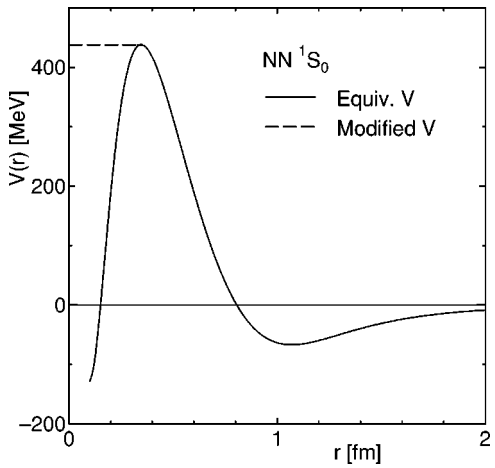

FIG. 11. Equivalent and modified local potential for the $NN\ ^1S_0$ channel in the OGEP quark model.

this channel, and that the potential may be simulated by the equivalent local potential, which has the same on-shell behavior.

Also, we investigate the effect of the short-range attractive pocket by performing a calculation without the pocket in the NN system. In Fig. 11, we show the modified local potential without the attractive pocket as well as the original equivalent local potential with the attractive pocket. The phase shifts given by both of the two potentials are shown in Fig. 12. From these figures, we understand that the modified potential gives the stronger repulsion at high energies. The difference between these phase shifts in the region from $k=3\ \mathrm{fm}^{-1}$ and higher produces the attractive pocket at short distances in the equivalent local potential.

In Figs. 13 and 14, we again investigate the nonlocality of the QCM potential in the $\Sigma N(T=3/2)\ ^3S_1$ channel by checking whether the contributions from each term are additive or not. As seen in the figures, the equivalent local potentials coming from each term shows the tendency to be additive. If we compare them with those for the $NN\ ^1S_0$ channel shown in Figs. 9 and 10, however, we see that additivity does not hold so well as in the $NN\ ^1S_0$ channel. This suggests that the nonlocality of the QCM potential is much higher in this channel.

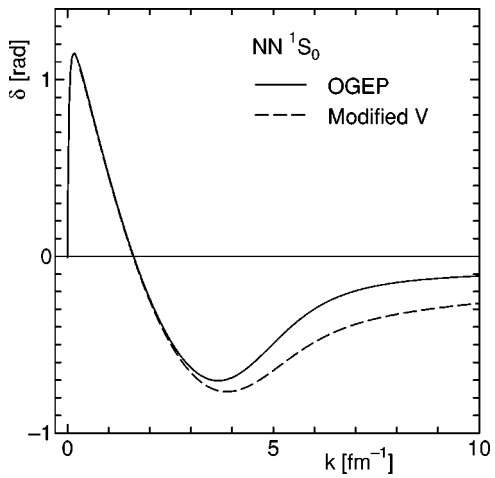

FIG. 12. Calculated phase shifts given by the equivalent and modified potentials for the $NN\ ^1S_0$ channel in the OGEP quark model.

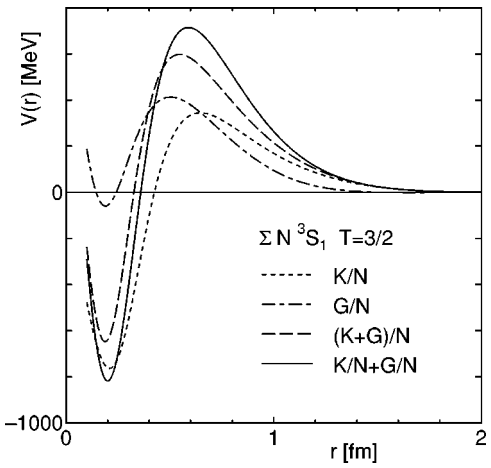

FIG. 13. Equivalent local potential for the $\Sigma N(T=3/2)\ ^3S_1$ channel in the OGEP quark model. For further explanations see Figs. 5 and 9.

VI. SUMMARY

In this paper, we have investigated the short-range part of the potential given by the quark cluster model, especially the quark Pauli-blocking effects and the nonlocal term coming from the quark potential. An energy-independent local potential can be reconstructed from a given phase shift by solving the inverse scattering problem. We have employed this method to derive the energy-independent local potential which reproduces the same phase shifts as those obtained from the QCM potential.

We have used two types of the quark cluster models. One is called the OGEP quark model, where the OGEP plays the dominant role to reproduce the mass difference between nucleon and Δ, and also to produce the NN short-range re-

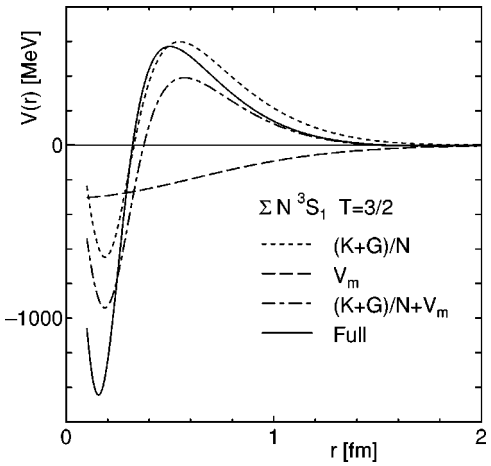

FIG. 14. Equivalent local potential for the $\Sigma N(T=3/2)\ ^3S_1$ channel in the OGEP quark model. For further explanations see Figs. 5 and 10.

pulsion. The other is the hybrid chiral quark model where the pseudoscalar- and scalar-meson-exchange potentials between quarks including quark exchanges are taken into account together with the OGEP. In the $NN\ {}^1S_0$ channel, once the peak value is fitted, there is almost no difference between these two models, but there appears a small difference in $\Sigma N(T=3/2)\ {}^3S_1$channel. Since there is no essential difference between these two models, we have restricted ourselves to the OGEP quark model to investigate the details of the potential derived from the quark model.

We have found that such an equivalent local potential has a strong repulsion at short distances in the $NN\ {}^1S_0$ in both quark models. We have, however, also found that there is an attractive pocket at very short distances. It is considered that such a pocket appears because the nonlocal repulsion becomes weaker effectively in the very-high-energy region. This repulsion-attractive-pocket structure becomes more manifest in the channel which has an almost-forbidden state, $\Sigma N(T=3/2)\ {}^3S_1$. There we have clarified the mechanism as to how the sharp increase of the phase shift occurs in connection with the norm kernel when there exists the almost-forbidden state. From the shape of the equivalent local potentials, it is clearly seen that the gluon exchange constructs the short-range repulsion in the $NN\ {}^1S_0$ while the quark Pauli-blocking effect governs the feature of the scattering phase shifts in the $\Sigma N(T=3/2)\ {}^3S_1$ channel.

ACKNOWLEDGMENTS

This work was supported in part by Grant-in-Aid for Scientific Research from JSPS (Nos. 11640258 and 12640290).

APPENDIX A: INVERSE SCATTERING PROBLEM

Here we briefly show how to derive an equivalent local potential from a given phase shift: Eqs. (18)–(21).

We assume that the S matrix is given by the extended Eckert potential

$$S(k)=\frac{g(k)+if(k)}{g(k)-if(k)}, \tag{A1}$$

$$\tan\delta(k)=f(k)/g(k), \tag{A2}$$

with

$$f(k)=k\sum_{m=0}^{n-1} f_m k^{2m}, \tag{A3}$$

$$g(k)=\sum_{m=0}^{n} g_m k^{2m}. \tag{A4}$$

The parameters n, $\{f_m\}$, and $\{g_m\}$ are determined so that this S matrix gives the given phase shift $\delta(k)$ up to about 15 fm^{-1}. Moreover, we use the condition, $g_n=1$, $f(k_0)=0$ at $\delta(k_0)=0$, etc., and f_n is determined to give the Born term,

$$f_n=-\frac{2\pi\mu}{\hbar^2}\langle V\rangle. \tag{A5}$$

By using this form of the S matrix, Eq. (18) becomes

$$F(r)=\frac{1}{2\pi i}\int_{-\infty}^{+\infty} e^{ikr}\frac{2f(k)}{g(k)-if(k)}dk+\sum_{\text{all }\kappa_j>0} c_j^2 e^{-\kappa_j r}. \tag{A6}$$

Because $g(k)-if(k)$ is the polynomial function of k of up to the $2n$th order, we have $2n$ poles at $k=t_i$ $(i=1-2n)$ in the integrand of the above equation in general. Thus, we have

$$F(r)=\sum_{\text{all }\Im t_m>0} Res\frac{2f(t_m)}{g(t_m)-if(t_m)}e^{it_m r}+\sum_{\text{all }\kappa_j>0} c_j^2 e^{-\kappa_j r}. \tag{A7}$$

So the equation to solve, Eq. (20), becomes a simple integral equation with the known function F, which can be solved numerically. The potential in Eq. (21) is derived directly from the kernel K.

The local potential which gives a given phase shift is uniquely determined. Since the systems we are concerned with in this paper do not have a bound state, the equivalent local potential can also be obtained by fitting the phase shift directly. We also use this fitting to check the above method. The reconstructed potentials by these two methods are similar to each other with a small numerical error, which cannot be distinguished in the figures.

APPENDIX B: MODEL FOR AN ALMOST-FORBIDDEN STATE

Here we explain a simplified model to investigate the mechanism of the role of an almost-forbidden state. This model is simplified in a way that the quark exchange does not occur among the ns $(n>0)$ states.

First we introduce a projection operator P which selects the $0s$ state:

$$P=|0s\rangle\langle 0s|.$$

Then we consider the one-body scattering problem given by the following normalization N and Hamiltonian H:

$$H\chi=EN\chi,$$

$$N=1-\alpha P,$$

$$H=T-\alpha(PT+TP)+\alpha PTP,$$

where T is the kinetic energy operator, E is the energy eigenvalue, and α is a parameter which is smaller than 1. When $\alpha=1$, the state $0s$ is called the forbidden state, and if α is close to 1, the state $0s$ is called the almost-forbidden state. Introducing the projection operator $Q=1-P$, we rewrite the N and H as follows:

$$N=Q+(1-\alpha)P,$$

$$H = QTQ + (1-\alpha)(QTP + PTQ + PTP).$$

This shows that the $0s$ state in the normalization N is reduced by a factor of $(1-\alpha)$ and the matrix elements of the Hamiltonian H between the $0s$ and ns states are also reduced by the factor of $(1-\alpha)$. Now let us calculate the H/N. When $\alpha<1$, $1/\sqrt{N}$ is given by

$$\frac{1}{\sqrt{N}} = Q + \frac{1}{\sqrt{1-\alpha}} P.$$

Then we obtain

$$\frac{1}{\sqrt{N}} H \frac{1}{\sqrt{N}} = QTQ + PTP + \sqrt{1-\alpha}(PTQ + QTP).$$

This tells us that only the nondiagonal matrix elements between the $0s$ and ns $(n \neq 0)$ are reduced by a factor of $\sqrt{1-\alpha}$. Therefore the state which contains a large part of the $0s$ component, namely, the low-energy scattering state, feels effectively a repulsion when the factor $\sqrt{1-\alpha}$ is smaller than 1.

[1] T. Hamada and I.D. Johnston, Nucl. Phys. **34**, 382 (1962).
[2] R.V. Reid, Jr., Ann. Phys. (N.Y.) **50**, 411 (1968).
[3] R. Machleidt, K. Holinde, and Ch. Elster, Phys. Rep. **149**, 1 (1987).
[4] M.M. Nagels, T.A. Rijken, and J.J. de Swart, Phys. Rev. D **15**, 2547 (1977); **15**, 2547 (1977); **20**, 1633 (1979).
[5] M. Oka and K. Yazaki, Phys. Lett. **90B**, 41 (1980); Prog. Theor. Phys. **66**, 556 (1981); **66**, 572 (1981).
[6] A. Faessler, F. Fernandez, G. Lübeck, and K. Shimizu, Phys. Lett. **112B**, 201 (1982); Nucl. Phys. **A402**, 555 (1983).
[7] M. Oka and K. Yazaki, in *Quarks and Nuclei*, edited by W. Weise (World Scientific, Singapore, 1985).
[8] K. Shimizu, Rep. Prog. Phys. **52**, 1 (1989).
[9] *Quark Cluster Model of Baryon-Baryon Interactions*, edited by M. Oka, K. Shimizu, and K. Yazaki [Suppl. Prog. Theor. Phys. **137**, 1 (2000))].
[10] Y. Suzuki and K.T. Hecht, Phys. Rev. C **27**, 299 (1983); **28**, 1458 (1983).
[11] M. Lacombe *et al.*, Phys. Rev. C **21**, 861 (1980).
[12] K. Shimizu and S. Yamazaki, Phys. Lett. B **390**, 1 (1997).
[13] M. Oka, K. Shimizu, and K. Yazaki, Nucl. Phys. **A464**, 700 (1987).
[14] S. Takeuchi, hep-ph/0008185.
[15] S. Takeuchi and K. Shimizu (unpublished).
[16] R.G. Newton, *Scattering Theory of Waves and Particles* (Springer-Verlag, New York, 1982).
[17] Z.S. Agranovich and V.A. Marchenko, *The Inverse Problem of Scattering Theory* (Gordon and Breach, New York, 1963).
[18] F.E. Close, *An Introduction to Quarks and Partons* (Academic, New York, 1988).
[19] N. Isgur and G. Karl, Phys. Lett. **72B**, 109 (1977); Phys. Rev. D **19**, 2653 (1979); **20**, 1191 (1979).
[20] A. De Rujula, H. Georgi, and S.L. Glashow, Phys. Rev. D **12**, 147 (1975).
[21] L.Ya. Glozman and D.O. Riska, Phys. Rep. **268**, 263 (1996).
[22] K. Shimizu and L.Ya. Glozman, Phys. Lett. B **477**, 59 (2000).
[23] M. Furuichi and K. Shimizu, Phys. Rev. C **65**, 025201 (2002).
[24] M.K. Srivastava, P.K. Banerjee, and D.W. Sprung, Phys. Lett. **29B**, 635 (1969).